



Case Report

Total talectomy and reconstruction using unrestricted 3D printed prosthesis for pediatric talus hemangioendothelioma

Yunlong Zhang, Zhichang Zhang^{*}

Department of Orthopedic Surgery, Shanghai Institute of Microsurgery on Extremities, Shanghai Sixth People's Hospital Affiliated to Shanghai Jiao Tong University School of Medicine, Shanghai, 200233, China

ARTICLE INFO

Keywords:

3D printed prosthesis
Unrestricted talus replacement
Pediatric

ABSTRACT

Background: Epithelioid hemangioendothelioma (EHE) is an ultra-rare vascular sarcoma with an extremely low incidence and prevalence, particularly in children. We report the case of a 9-year-old girl diagnosed with EHE. There are limited reconstruction methods available following total talus resection for vascular endothelioma of the talus, and the use of a 3D-printed talus prosthesis in pediatric cases has not been previously documented.

Case presentation: A 9-year-old girl presented to our unit with swelling, pain, and limited mobility of the ankle for one month without an obvious cause. X-ray and CT imaging revealed osteolytic lesions in the talus, which was identified as a low-grade malignant tumor that had nearly completely invaded the talus and was surrounded by immature bone. The American Foot and Ankle Surgery Association (AOFAS) score was 75/100. We performed a total resection of the talus followed by unrestricted talus replacement. Three months post-operation, the child was able to walk unaided. Ankle function was assessed at 6 and 13 months post-surgery, with the AOFAS score improving from 75 to 91, indicating that her functional needs for daily life were largely met.

Conclusion: Following complete excision of the lesion, the immature bone surrounding the talus was successfully preserved using an unrestricted 3D-printed prosthesis during ankle reconstruction. Our patient demonstrated satisfactory ankle function during the 6-month follow-up. This method is both safe and stable, yielding promising results, particularly for juvenile patients.

1. Introduction

Epithelioid hemangioendothelioma (EHE) is an ultra-rare, translocated vascular sarcoma primarily located in the lung, liver, soft tissue, and bone of the lower limb. It is characterized as a low-grade malignant tumor that causes expansive osteolytic destruction. The incidence of EHE is approximately 0.038 per 100,000 individuals per year, with a prevalence of less than 1 per 1,000,000 (Lau et al., 2011; Stacchiotti et al., 2021a; De Pinieux et al., 2021), exhibiting a slight predominance in women. The incidence peaks during the fourth to fifth decades of life, and EHE is exceedingly rare in children (Rosenbaum et al., 2020; Guo et al., 2017; Flucke et al., 2014). When EHE affects the bones, the axial skeleton and lower limbs are the most commonly involved sites. Bone lesions are typically poorly demarcated and lytic, with some presenting a sclerotic rim at initial diagnosis (Stacchiotti et al., 2021b). For bony EHE, surgical resection should strive for microscopic negative margins, involving en bloc resection of the bone of origin along with the affected

soft tissues (Casali et al., 2018).

Currently, several alternative management options exist for malignant tumors of the talus, including below-knee amputation, tibio-calcaneal arthrodesis, and homogeneous bone transplantation; however, these approaches have limitations that restrict their clinical application. The use of a three-dimensional (3D) printed total talus prosthesis for talus lesions represents an effective method for talar reconstruction.

In this report, we present an alternative limb-sparing surgical approach for the management of pediatric talus hemangioendothelioma, utilizing a 3D-printed talar prosthesis for replacement.

2. Case presentation

A 9-year-old girl (height: 145 cm, weight: 42 kg) was admitted to our unit due to swelling, pain, and limited mobility without an obvious cause for one month.

Physical examination revealed a palpable mass in front of the ankle,

^{*} Corresponding author at: Department of Orthopedic Surgery, Shanghai Institute of Microsurgery on Extremities, Shanghai Sixth People's Hospital Affiliated to Shanghai Jiao Tong University School of Medicine, 600 Yishan Road, Shanghai, 200233, China.

E-mail address: zcc163mail@163.com (Z. Zhang).

<https://doi.org/10.1016/j.bonr.2025.101830>

Received 8 September 2024; Received in revised form 13 December 2024; Accepted 12 February 2025

Available online 13 February 2025

2352-1872/© 2025 Published by Elsevier Inc. This is an open access article under the CC BY-NC-ND license (<http://creativecommons.org/licenses/by-nc-nd/4.0/>).

mild tenderness, normal skin temperature, palpable distal blood flow and sensation, and slightly restricted movement of the left ankle. By reviewing her medical history, we excluded trauma, surgical intervention, familial inheritance, infection, hormonal factors, and rheumatoid conditions. Preoperative ankle function was primarily characterized by limited dorsiflexion, with an AOFAS score (American Orthopedic Foot & Ankle Society) of 75 out of 100. X-ray and CT images of the ankle demonstrated osteolytic lesions of the talus, with marginal sclerosis not being prominent, local cortical discontinuity in front of the talus, and a reactive soft tissue mass (Fig. 1 A, B). Enhanced MRI of the ankle revealed slightly low signal intensity on T1-weighted imaging (T1WI) (Fig. 1 C, F), uneven high signal intensity on T2-weighted imaging (T2WI) and fat suppression sequences, uneven enhancement of the lesion, a soft tissue mass surrounding the talus, and significant edema with poorly defined boundaries (Fig. 1 D, E). The bone scan confirmed the absence of distant metastasis. To further clarify the diagnosis, a talus puncture biopsy was performed, and the pathological analysis indicated epithelioid hemangioendothelioma (Fig. 2).

The lesion was identified as a low-grade malignant tumor that had nearly completely invaded the talus, which was surrounded by immature bone. Consequently, we opted for a total resection of the talus followed by unrestricted talus replacement. The design of the prosthesis was based on 3D printed data obtained from CT scans of the healthy contralateral talus (Fig. 3) (Fig. 4 A-D). The 3D-printed prosthesis was sterilized using ethylene oxide gas sterilization. This method was chosen because it is effective in killing microorganisms while maintaining the integrity of the prosthesis material. The prosthesis was packaged and labeled according to standard sterilization procedures.

Under general anesthesia, the patient was placed in the supine position. A standard anterolateral ankle approach was used to dissect the soft tissue to fully expose the talus, and the ligaments connected to the talus were carefully dissected and marked for subsequent reconstruction operations. The talus was excised en bloc to ensure clear resection margins. The tibial part of the 3D printed prosthesis was inserted into the tibial fossa, and the calcaneus part was fixed on the calcaneus with screws. The upper part of the prosthesis was chosen with high molecular weight polyethylene based on its excellent wear resistance, which would reduce wear between the implant and the tibiofibula over time. The titanium alloy was selected for the lower part, which has high strength and good biocompatibility to ensure the long-term stability and safety of the prosthesis. These materials have been widely used in orthopedic implants. The tenon and mortise on the prosthesis are precisely inserted into the carefully prepared groove of the adjacent bone, and the tenon fits closely to the groove to form a firm interlocking connection. Check and clean the groove before insertion, tap the prosthesis to make it in place after insertion, and clamp the groove inside to further enhance stability and effectively prevent micro-movement of the prosthesis. The fixation effect was tested during the operation to ensure that the prosthesis could withstand the normal physiological load. The suture holes of the prosthesis were strategically placed at the corresponding insertion points of the talar ligament, such as three suture holes on the anterior part of the talofibular ligament prosthesis, two suture holes on the internal side of the deltoid ligament prosthesis, and two suture holes on the posterior part of the talofibular ligament prosthesis. Non-absorbable suture passes through the stump of the ligament and the suture hole of the prosthesis, tightening and binding the ligament, and restoring

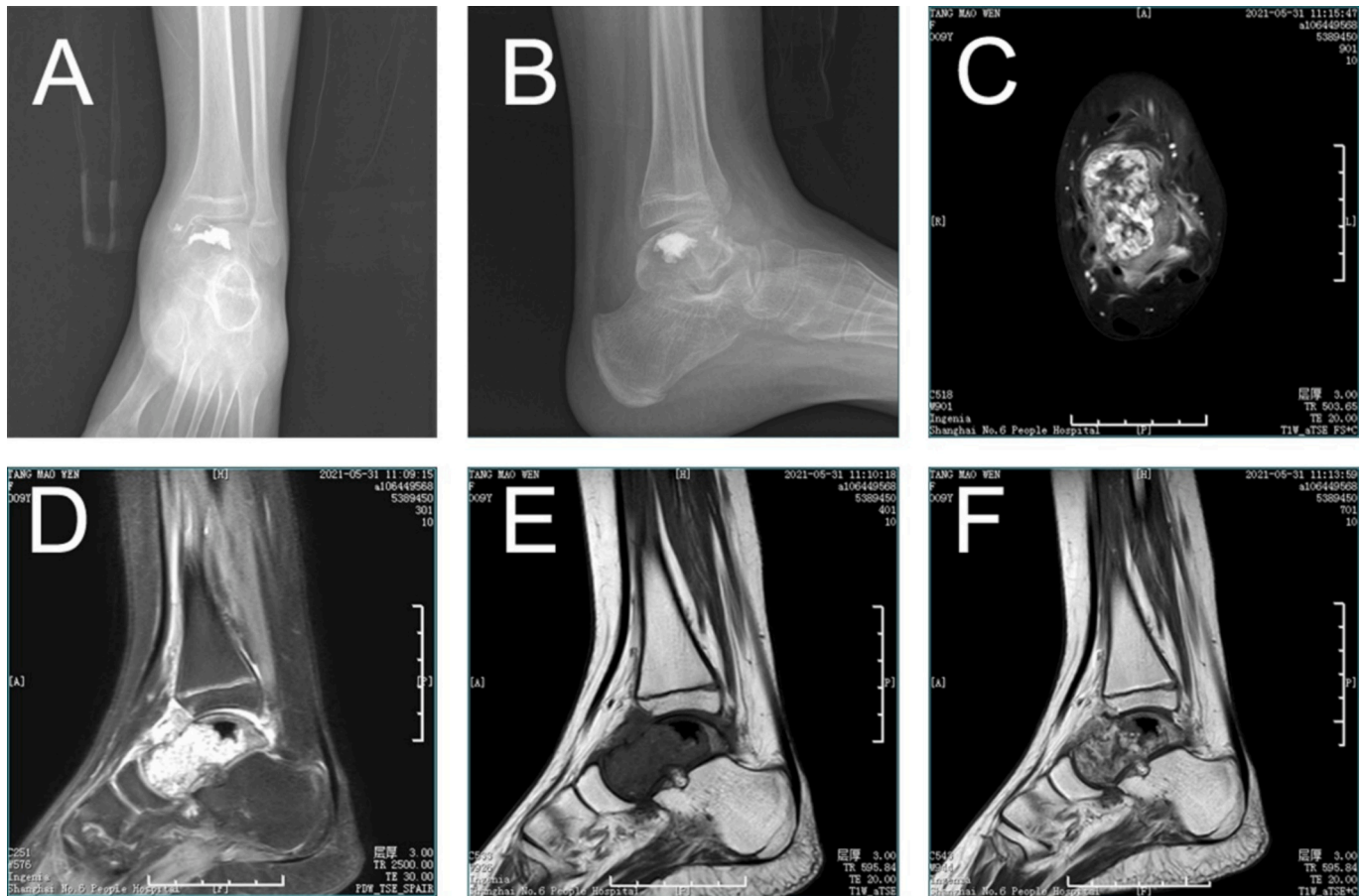


Fig. 1. Imaging findings at presentation. (A,B) preoperative X-ray Radiographs. The ankle showed osteolytic lesions of the talus, marginal sclerosis was not obvious, local cortical discontinuity in front of the talus, and reactive soft tissue mass was formed. Magnetic resonance imaging findings of the ankle (C, F) Enhanced T1-weighted images. Enhanced MRI of the ankle showed slightly low signal intensity on T1WI, uneven enhancement of the focus, soft tissue mass around the talus, obvious edema and unclear boundary. (D)T2-weighted images. Uneven high signal intensity on T2WI and fat suppression sequence. (E)T1-weighted images.

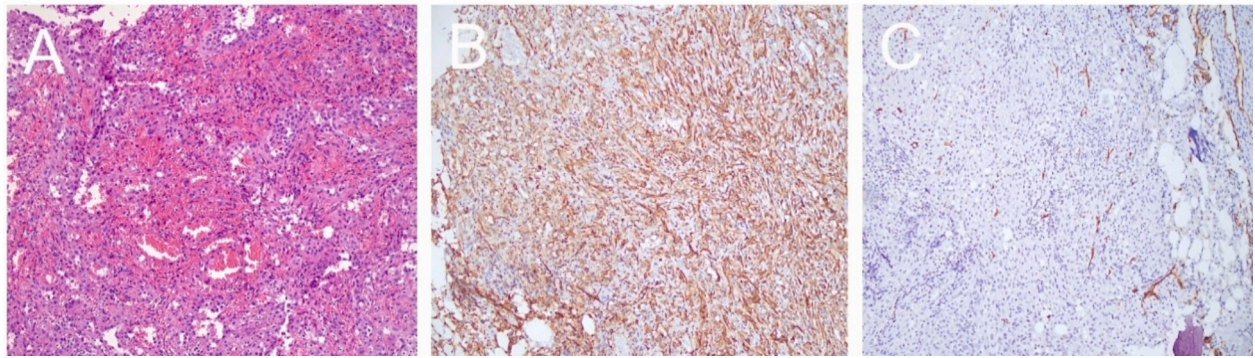


Fig. 2. Histopathological features of the tumor. (A) Hematoxylin and eosin staining shows the tumor cells arranged in cords and nests, with a myxoid stroma. HE \times 200 (B) Immunohistochemical staining for CD31 shows positive expression in the tumor cells, confirming the endothelial origin. Envision \times 200 (C) Immunohistochemical staining for CD34 also shows positive expression in the tumor cells. Envision \times 200.

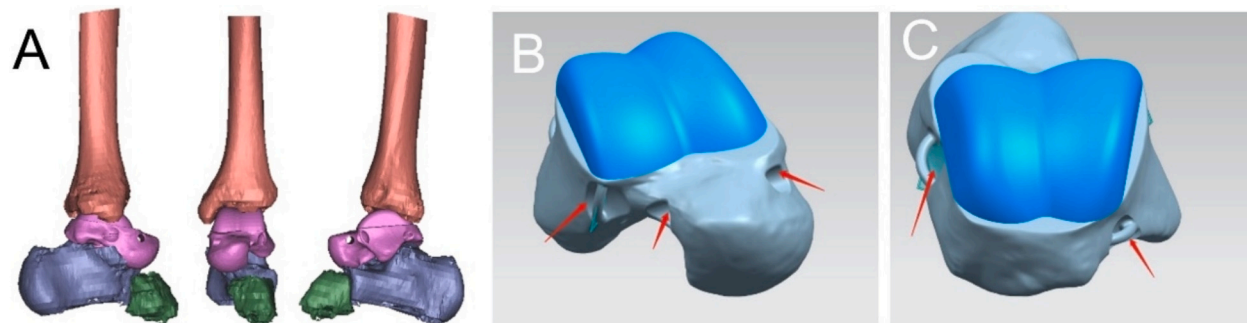


Fig. 3. Preoperative planning images. (A) Refers to the CT images of the contralateral healthy ankle joint, and the 3D data of the affected ankle joint are reconstructed symmetrically. (B,C) The upper part of the talus with a large range of motion is made of polyethylene material (blue part in the figure) to protect the articular cartilage around the prosthesis. The lower part of the talus was made of titanium alloy (silver part in the figure). According to the attachment point of the talus ligament, the suture hole (red arrow) was designed to facilitate intraoperative ligament reconstruction.

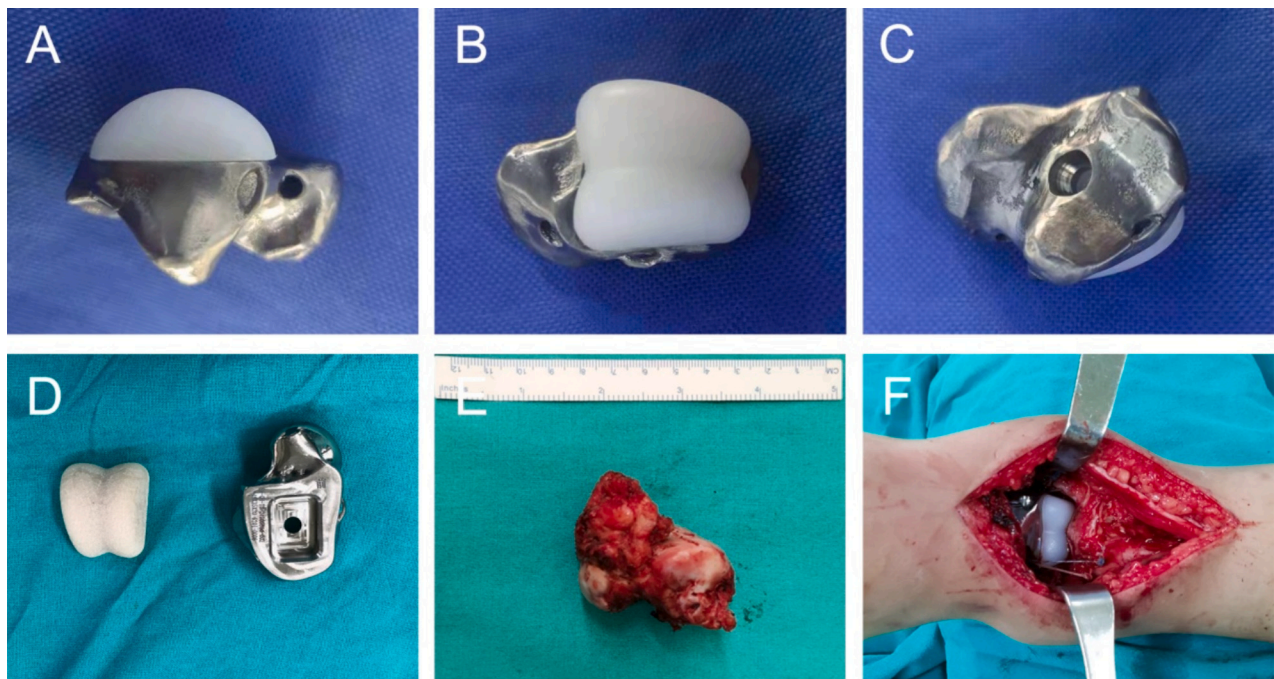


Fig. 4. Prosthesis and implantation. (A-D) prosthesis photos. (E) complete resection of the lesion during operation. (F) prosthesis implantation during operation

normal tension and stability of the ankle joint. After talus resection, the soft tissue was thoroughly examined for injury, and the necrotic or injured soft tissue was demineralized to promote healing and prevent infection. The soft tissue was re-approached and sutured in layers to provide good coverage and support for the prosthesis and complete the operation. The total duration of this procedure was approximately 96 min, and the blood loss was approximately 150 ml (Fig. 4E,F).

Postoperative pathology results were consistent with the findings from the initial puncture pathology. The wound healed well, and the ankle joint was immobilized in plaster for six weeks. During this time, we asked the patient to keep the leg elevated to reduce swelling. After 6 weeks, the cast was removed and partial weight-bearing exercise was gradually started under the guidance of a physical therapist. The physical therapist also provided instructions regarding range of motion exercises to improve ankle flexibility. The physical therapy program consisted of a progressive program. In the initial stage, gentle range of motion exercises, including ankle dorsiflexion, plantarflexion, varus, and valgus, were performed after removal of the cast. As the patient improved, resistance exercises were added to strengthen the ankle muscles. These movements include the use of elastic bands and a heel lift. Balance training is also an important part of the program, with patients standing on one leg and performing various balance tasks. The physical therapist adjusts the intensity and frequency of exercise according to the patient's progress and tolerance. At 12 weeks after surgery, the patient was allowed to bear full weight and continued a home exercise program to maintain and improve ankle function. Three months following the operation, the child was able to walk independently. Ankle function was assessed at six months (Fig. 5) and thirteen months (Fig. 6) postoperatively, with the AOFAS score improving from 75 to 91, thereby adequately meeting the requirements for daily activities. Weight-bearing ankle radiographs indicated that the prosthesis was well-positioned in relation to the contralateral joint. The range of motion of the ankle joint in the directions of plantarflexion, varus and valgus were measured during the follow-up, and the range of motion of the ankle joint was compared with that of normal children. The results showed that the range of motion of the ankle joint gradually improved

with time, and it was close to the normal range at 13 months after operation, which further proved the effectiveness of the surgical method. At 3 years after operation (Fig. 7), the X-ray films of the ankle joint showed good position and stable prosthesis. The ankle function score was similar to the previous one, and there was no obvious ankle instability and pain after walking. The distal tibial articular surface of the patient was effectively protected without obvious bone destruction. Compared with the initial operation, the epiphysis of the patient had developed normally and no leg length discrepancy occurred, which also met our preoperative expectation and established a good foundation for the subsequent ankle revision surgery.

3. Discussion

EHE is an exceptionally rare vascular sarcoma, with an estimated prevalence of less than one in a million individuals. It originates from precursor cells that exhibit endothelial characteristics and specific fusion genes (Flucke et al., 2014; Tanas et al., 2011; Errani et al., 2011; Choi and Ro, 2021). Although EHE has a peak incidence in middle age, it can also affect a wide age range, including children (Cournoyer et al., 2020; Orbach et al., 2022) (Table 1).

EHE of bone typically presents as multicentric lesions (Weissferdt and Moran, 2014), with more than half of these cases occurring in the lower extremities. For surgical treatment, wide resection or an intralesional procedure is preferred for localized disease when feasible, and these approaches appear to be reasonable options for most EHE cases in the lower extremity (Angelini et al., 2014). While lesions in the distal lower extremity are often best treated surgically with amputation, this approach can be considered drastic for low-grade disease. Kumar et al. (2015). reported a case of multicentric EHE in an adult involving the talus and tibia; the tumor was excised, and ankle arthrodesis was performed, with a fibular graft placed in the defect area. The patient was doing well at one-year follow-up. Additionally, Chaudhary et al. (2022). documented a case of a giant cell tumor of the talus in a 17-year-old female, where talectomy followed by calcaneo-tibial fusion was performed, as intralesional curettage was not feasible. Tibiocalcaneal fusion

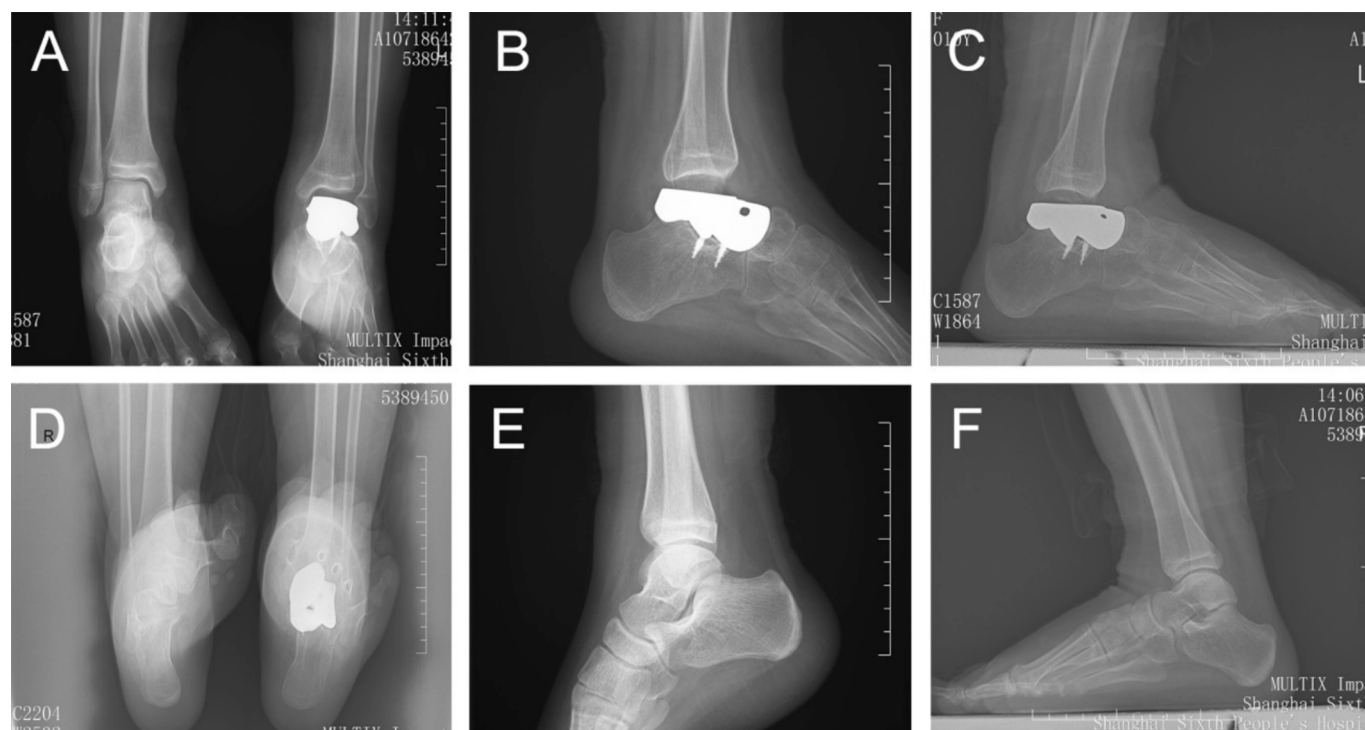


Fig. 5. X-ray evaluation 6 months after surgery. (A) bilateral anteroposterior radiographs. (B,E) bilateral non-weight-bearing lateral radiographs. (C,F) bilateral weight-bearing lateral radiographs. (D) bilateral axial radiographs of calcaneus

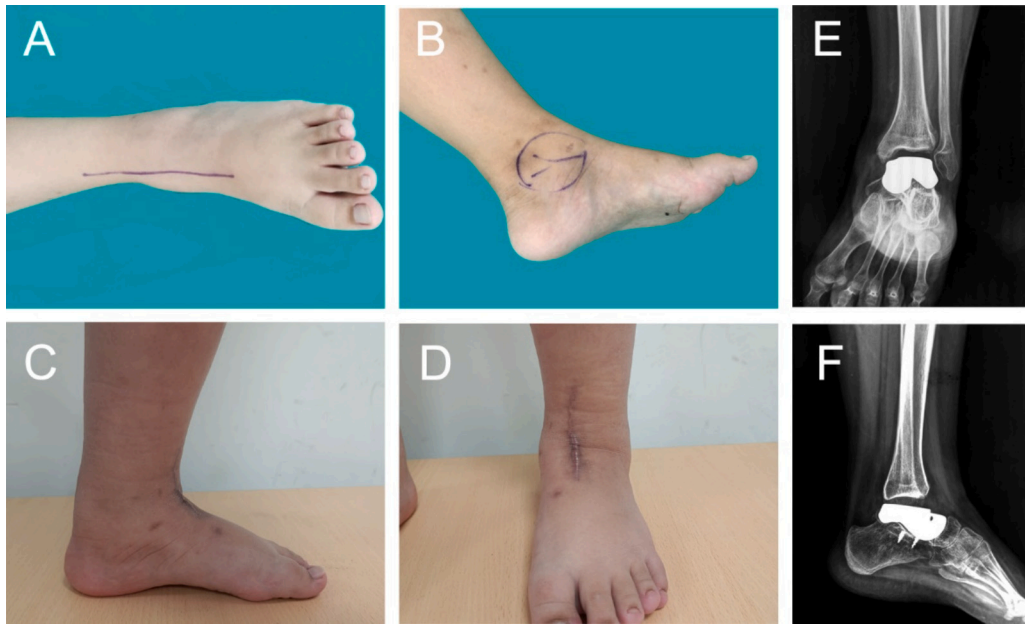


Fig. 6. Preoperative and postoperative photos. (A,B) before surgery. (C,D) 6 months after surgery. (E,F) X-ray evaluation after surgery. 13 months after surgery



Fig. 7. The X-ray films were reviewed 3 years after operation. (A) Lateral radiographs. (B) anteroposterior radiographs.

Table 1

Supplement of previous case reports or overviews of pediatric hemangioendothelioma case series.

Authors	Number of cases	Location of the tumor	Treatment method	Follow-up result
Cournoyer et al. (2020)	14	Multiple sites (including bone)	Surgical resection, chemotherapy	5-year survival rate: 86 %
Orbach et al. (2022)	23	Bone (including talus)	Surgery, chemotherapy, radiotherapy	Overall survival rate: 87 % at 5 years
Kumar et al. (2015)	1	Tibia and talus	Excision and ankle arthrodesis	Good function at 1-year follow-up
Chaudhary et al. (2022)	1	Talus	Talectomy and calcaneo-tibial fusion	Able to bear weight with orthosis

was accomplished using an external fixator, which was removed after three months, and the patient was advised to engage in full weight-bearing activities while using an ankle-foot orthosis. In this study, the customized 3D-printed implant successfully reconstructed the talus both

functionally and anatomically. Additionally, the talar prosthesis utilized during the surgery significantly reduced surgical time, eliminated the need for intraoperative fluoroscopy, reconstructed the ligaments surrounding the talus, and facilitated excellent walking ability without support. Unlike traditional reconstruction techniques, this approach does not face limitations such as restricted soft tissue coverage of the bone, a high incidence of complications, or the necessity for complete bone union. However, limb-sparing surgery using a 3D-printed implant for tumors located on the talus does present certain challenges. First, achieving a sound oncological margin of resection for effective local tumor control is more difficult with 3D-printed implants compared to below-the-knee amputation. Second, the high cost of the prosthesis may restrict its broader application. Finally, the presence of the metal implant may complicate the detection of local tumor recurrence on the talus through CT scanning or MRI.

Given that this patient is a child, we are aware of the potential effect of growth on long-term outcomes. 3D printed prostheses are designed with some flexibility to accommodate potential growth. However, we also recognize that continuous monitoring of patient growth and prosthesis fitness is necessary. Future research should focus on developing more growth-friendly prosthesis design and monitoring strategies to ensure optimal treatment outcomes for pediatric talus tumor patients. Patients will undergo long-term monitoring to assess the durability and function of the prosthesis. This will include regular clinical examinations every 6 months to assess ankle function, range of motion, and gait. Radiological evaluation, including X-ray and CT scan, if necessary, was performed annually to detect any signs of prosthesis loosening, wear, or tumor recurrence. Growth plate assessment will continue until the patient reaches skeletal maturity. Patients will be asked to report any new or worsening symptoms such as pain, swelling, or limited ankle motion. At each follow-up visit, the wound site will be examined for signs of infection or inflammation, closely monitored for any potential complications, and any complications identified will be managed according to established protocols, including conservative treatment, revision surgery, or other appropriate interventions.

Given the rarity of the disease, large studies evaluating treatment strategies are limited. Furthermore, reconstruction options have not been widely discussed (Rosenberg and Agulnik, 2018). To the best of our knowledge, this is the first report on the use of unrestricted 3D-printed prostheses for pediatric talus hemangioendothelioma.

4. Conclusion

In conclusion, we present an innovative limb-sparing surgical approach for managing pediatric talus hemangioendothelioma, utilizing a 3D-printed talar prosthesis for replacement. Our findings indicate that the functional and clinical outcomes associated with the 3D-printed implant surpass those of traditional methods, including autografts, allografts, and amputation. This technique not only resulted in fewer complications but also addressed several limitations inherent in autografts and allografts, as well as amputation. Our experience suggests that 3D-printed implants represent a viable option for patients with tumors of the talus. It is important to note that any patient diagnosed with cancer requires comprehensive oncology management; thus, the surgical intervention described herein serves as an adjunct to the patient's overall care plan.

We believe this is the first report globally documenting total resection of a pediatric talus tumor followed by reconstruction using an unrestricted 3D-printed talar prosthesis. This surgical technique holds promising potential for application, particularly in juvenile patients. We anticipate that further studies will be conducted to elucidate the indications for this technique, and that a comprehensive summary of our experiences and technical enhancements will emerge with extended follow-up.

CRedit authorship contribution statement

Yunlong Zhang: Writing – review & editing, Writing – original draft, Conceptualization. **Zhichang Zhang:** Writing – review & editing, Conceptualization.

Ethics statement

The study was approved by “Shanghai Sixth People's Hospital” research ethical committee. Written informed consent was obtained from the individual(s) for the publication of any potentially identifiable images or data included in this article.

Funding statement

The authors did not receive any outside funding or grants in support of their research for or preparation of this work.

Declaration of competing interest

The authors declare that they have no known competing financial interests or personal relationships that could have appeared to influence the work reported in this paper.

Acknowledgments

We thank the patient for the participation and Editage (www.editage.com) for English-language editing.

Data availability

Data will be made available on request.

References

- Angelini, A., Mavrogenis, A.F., Gambaretto, M., Merlino, B., Picci, P., Ruggieri, P., 2014. Surgical treatment and results of 62 patients with epithelioid hemangioendothelioma of bone. *J. Surg. Oncol.* 109 (8), 791–797.
- Casali, P.G., Abecassis, N., Aro, H.T., Bauer, S., Biagini, R., Bielack, S., et al., 2018. Soft tissue and visceral sarcomas: ESMO-EURACAN clinical practice guidelines for diagnosis, treatment and follow-up. *Annals of oncology : official journal of the European society for. Med. Oncol.* 29(Suppl 4):iv51-iv67.
- Chaudhary, S.D., Agrawal, P.S., Sakthar, N.S., 2022. Giant cell tumor of talus: a case report. *J. Orthopaedic Case Rep.* 12 (9), 92–94.
- Choi, J.H., Ro, J.Y., 2021. The 2020 WHO classification of tumors of soft tissue: selected changes and new entities. *Adv Anat Pathol* 28 (1), 44–58.
- Cournoyer, E., Al-Ibraheemi, A., Engel, E., Chaudry, G., Stapleton, S., Adams, D.M., 2020. Clinical characterization and long-term outcomes in pediatric epithelioid hemangioendothelioma. *Pediatr. Blood Cancer* 67 (2), e28045.
- De Pinieux, G., Karanian, M., Le Loarer, F., Le Guellec, S., Chabaud, S., Terrier, P., et al., 2021. Nationwide incidence of sarcomas and connective tissue tumors of intermediate malignancy over four years using an expert pathology review network. *PLoS One* 16 (2), e0246958.
- Errani, C., Zhang, L., Sung, Y.S., Hajdu, M., Singer, S., Maki, R.G., et al., 2011. A novel WWTR1-CAMTA1 gene fusion is a consistent abnormality in epithelioid hemangioendothelioma of different anatomic sites. *Genes Chromosomes Cancer* 50 (8), 644–653.
- Flucke, U., Vogels, R.J., de Saint Aubain Somerhausen, N., Creyten, D.H., Riedl, R.G., van Gorp, J.M., et al., 2014. Epithelioid Hemangioendothelioma: clinicopathologic, immunohistochemical, and molecular genetic analysis of 39 cases. *Diagn. Pathol.* 9, 131.
- Guo, Q., Xue, J., Xu, L., Shi, Z., Zhou, B., 2017. The clinical features of epithelioid hemangioendothelioma in a Han Chinese population: a retrospective analysis. *Medicine* 96 (26), e7345.
- Kumar, D., Jain, V.K., Bhardwaj, M., Naik, A.K., Nasa, R., Arya, R.K., 2015. Epithelioid hemangioendothelioma of tibia and talus: a case report. *Oman Med. J.* 30 (4), 295–298.
- Lau, K., Massad, M., Pollak, C., Rubin, C., Yeh, J., Wang, J., et al., 2011. Clinical patterns and outcome in epithelioid hemangioendothelioma with or without pulmonary involvement: insights from an internet registry in the study of a rare cancer. *Chest* 140 (5), 1312–1318.
- Orbach, D., Van Noesel, M.M., Brennan, B., Corradini, N., Alaggio, R., Ben Arush, M., et al., 2022. Epithelioid hemangioendothelioma in children: the European pediatric soft tissue sarcoma study group experience. *Pediatr. Blood Cancer* 69 (10), e29882.
- Rosenbaum, E., Jadeja, B., Xu, B., Zhang, L., Agaram, N.P., Travis, W., et al., 2020. Prognostic stratification of clinical and molecular epithelioid hemangioendothelioma subsets. *Modern pathology : an official journal of the United States and Canadian Academy of Pathology, Inc.* 33 (4), 591–602.
- Rosenberg, A., Agulnik, M., 2018. Epithelioid hemangioendothelioma: update on diagnosis and treatment. *Curr. Treat. Options Oncol.* 19 (4), 19.
- Stacchiotti, S., Frezza, A.M., Blay, J.Y., Baldini, E.H., Bonvalot, S., Bovée, J., et al., 2021a. Ultra-rare sarcomas: a consensus paper from the Connective Tissue Oncology Society community of experts on the incidence threshold and the list of entities. *Cancer* 127 (16), 2934–2942.
- Stacchiotti, S., Miah, A.B., Frezza, A.M., Messiou, C., Morosi, C., Caraceni, A., et al., 2021b. Epithelioid hemangioendothelioma, an ultra-rare cancer: a consensus paper from the community of experts. *ESMO Open* 6 (3), 100170.
- Tanas, M.R., Sboner, A., Oliveira, A.M., Erickson-Johnson, M.R., Hespelt, J., Hanwright, P.J., et al., 2011. Identification of a disease-defining gene fusion in epithelioid hemangioendothelioma. *Sci. Transl. Med.* 3(98):98ra82.
- Weissferdt, A., Moran, C.A., 2014. Epithelioid hemangioendothelioma of the bone: a review and update. *Adv Anat Pathol* 21 (4), 254–259.